

Quantum Chemical and FTIR Spectroscopic Studies on the Linkage Isomerism of Carbon Monoxide in Alkali-Metal-Exchanged Zeolites: A Review of Current Research

C. Otero Areán^{1*}, G. Turnes Palomino¹, A. A. Tsyganenko², E. Garrone³

¹ Departamento de Química, Universidad de las Islas Baleares, 07071 Palma de Mallorca, Spain

*E-mail: dqueep0@clust.uib.es

² Institute of Physics, St. Petersburg University, 198504 St. Petersburg, Russia

³ Dipartimento di Scienza dei Materiali ed Ingegneria Chimica, Politecnico di Torino, 10129 Turin, Italy

Received: 21 May 2002 / Accepted: 13 June 2002 / Published: 31 July 2002

Abstract: When adsorbed (at a low temperature) on alkali-metal-exchanged zeolites, CO forms both $M(\text{CO})^+$ and $M(\text{OC})^+$ carbonyl species with the extra-framework alkali-metal cation of the zeolite. Both quantum chemical and experimental results show that C-bonded adducts are characterized by a C–O stretching IR band at a frequency higher than that of 2143 cm^{-1} for free CO, while for O-bonded adducts this IR band appears below 2143 cm^{-1} . The cation-CO interaction energy is higher for $M(\text{CO})^+$ than for $M(\text{OC})^+$ carbonyls, although the corresponding difference decreases substantially when going from Li^+ to Cs^+ . By means of variable-temperature FTIR spectroscopy, this energy difference was determined for several alkali-metal cations, and the existence of a thermal equilibrium between $M(\text{CO})^+$ and $M(\text{OC})^+$ species was established. The current state of research in this field is reviewed here, with a view to gain more insight into the thermal isomerization process.

Keywords: Alkali metal carbonyls, CO adsorption, FTIR spectroscopy, Linkage isomerism, Zeolites.

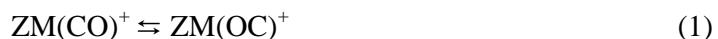
1. Introduction

Molecules confined within the channels and cavities of cation-exchanged zeolites are exposed to strong electrostatic fields created by extra-framework cations and neighbouring framework anions. These electric fields bring about polarization of the adsorbed molecule which thus finds its electron distribution significantly altered, and hence its reactivity [1,2]. Interaction of adsorbed molecules with extra-framework cations is a key factor controlling intrazeolite chemistry (including catalytic chemical processes) and it is also the base for several technical applications of zeolites, such as drying, air separation (oxygen from nitrogen) and the removal of contaminants from the atmosphere or from natural gas, to name only a few examples. Detailed characterization of the physico-chemical processes occurring upon interaction of guest molecules with zeolites is a prime requirement to understand chemical reactivity and it would also help to improve zeolite-based technology. Regarding carbon monoxide, clear understanding of the interaction between this molecule and zeolites is also of considerable interest in zeolite characterization [2], since CO is a widely used probe molecule for infrared spectroscopic studies of zeolites and related materials [3-20].

Infrared spectra of CO adsorbed (usually at a low temperature) on alkali-metal-exchanged zeolites invariably show a main IR absorption band upward shifted with respect to the 2143 cm^{-1} value of free CO. The magnitude of the corresponding hypsochromic shift depends on the extra-framework cation and on the number of neighbouring framework anions. Thus, for the series of M^+ -ZSM-5 zeolites ($\text{M} = \text{Li, Na, K, Rb, Cs}$) this cation-specific high frequency (HF) band was observed at wavenumbers which increase gradually from 2157 cm^{-1} for Cs^+ up to 2195 cm^{-1} for Li^+ [19,21]. The influence of framework anions is neatly shown by the fact that in Na-ZSM-5 the corresponding C–O stretching band appears at 2178 cm^{-1} [21], while in Na-Y the band maximum occurs at 2171 cm^{-1} [13]. Both, experimental results and theoretical calculations [9,13,22,23] show that this HF band corresponds to the fundamental C–O stretching mode of carbon monoxide polarized by the electrostatic field created by the cation (and nearby framework anions) in $\text{M}^+\cdots\text{CO}$ adducts. Besides the HF band, a weaker low frequency (LF) band was also frequently noted [24-27] in the infrared spectra of alkaline zeolites containing adsorbed CO. This LF band, which appears below 2143 cm^{-1} , is also cation specific; for the M^+ -ZSM-5 series it was observed at wavenumbers gradually increasing from 2100 cm^{-1} for Li^+ [19] up to 2122 cm^{-1} for Cs^+ [21]. In agreement with recent quantum-chemical calculations for CO interacting with both bare cations [23,28] and $\text{AlH}(\text{OH})_3\text{M}^+$ clusters [29] used to simulate cations in zeolites, the LF band must be assigned to the fundamental C–O stretching mode of $\text{M}^+\cdots\text{OC}$ adducts. Note that, because of its dipolar character, interaction of the CO molecule with a positively charged centre through the oxygen atom results in a lowering of the C–O stretching frequency (relative to free CO), while an increase should be expected for an interaction through the carbon atom [30,31].

Alkali metal $\text{M}(\text{CO})^+$ carbonyls are among those recently termed [32] *nonclassical metal carbonyls*, and they have considerable interest for both theoretical studies and experimental research. Variable-temperature FTIR spectroscopy has shown [33] that $\text{M}(\text{CO})^+$ species, formed by interaction

between CO and alkali metal exchanged zeolites, are inter-related to $M(OC)^+$ species by an isomerization equilibrium which can be described by the equation:



where Z stands for the zeolite framework and M is an extra-framework cation. Therefore, C-bonded and O-bonded adducts represent a case of linkage isomerism.

Initial work on the CO/Na-ZSM-5 system [33] has recently been extended to other alkali-metal-exchanged ZSM-5 zeolites [34,35], as well as to the faujasite-type Na-Y zeolite [36]. From the combination of experimental measurements [33-36] with quantum chemical calculations [23,28,29] it is becoming increasingly clear that the enthalpy change involved in the isomerization equilibrium described by equation (1) depends on both the cation involved and the zeolite structure type. The evidence so far available is examined here, with a view to derive a more detailed understanding than what can be obtained by considering individual cases alone.

2. Summary of experimental procedures and results

Na-ZSM-5 (Si/Al= 25) and Na-Y (Si/Al= 2.5) zeolites were synthesized following standard methods [37]. From the original Na-ZSM-5 sample, K-ZSM-5 and Rb-ZSM-5 were obtained by ion exchange with appropriate solutions of the corresponding metal nitrates. For IR spectroscopic studies, a thin self-supported wafer of each sample was prepared and outgassed (activated) in a dynamic vacuum (residual pressure $< 10^{-4}$ Torr) for 2 h at about 700 K inside an infrared cell which allowed in situ high-temperature activation, gas dosage, and variable-temperature spectroscopic measurements to be carried out. Details on the design and performance of this home-made infrared cell can be found elsewhere [38]. Liquid nitrogen was used for refrigeration and temperature was measured by means of a platinum resistance thermometer inserted close to the zeolite wafer. For better thermal contact between the sample wafer and the refrigerated cell, 0.3 Torr of helium was admitted into the sample compartment before running the background spectrum at liquid nitrogen temperature. Carbon monoxide was then dosed to an equilibrium pressure of 1 to 2 Torr, the cell was closed and infrared spectra were recorded at 77 K and on gradual warming up of the infrared cell following removal of liquid nitrogen. Series of transmission IR spectra, at 2 cm^{-1} resolution, were thus taken at about 10 K intervals in the range going from 77 K to room temperature.

Figure 1 shows some selected variable-temperature IR spectra of CO adsorbed on Na-ZSM-5. The HF band, corresponding to $Na^+ \cdots CO$ adducts, is observed at 2178 cm^{-1} . The LF band, due to $Na^+ \cdots OC$ species, appears at 2112 cm^{-1} . At 77 K the intensity of this LF band was extremely low [36]. However, on gradually raising the temperature, when the intensity of the HF band starts to decrease the LF band increases: spectra 1 to 3 in Figure 1. At higher temperatures (spectra 4 to 6) both bands decrease, because the net amount of CO which remains adsorbed decreases rapidly. However, the ratio of integrated intensities A_{LF}/A_{HF} was found to increase continuously over the whole temperature range, from 77 to 303 K.

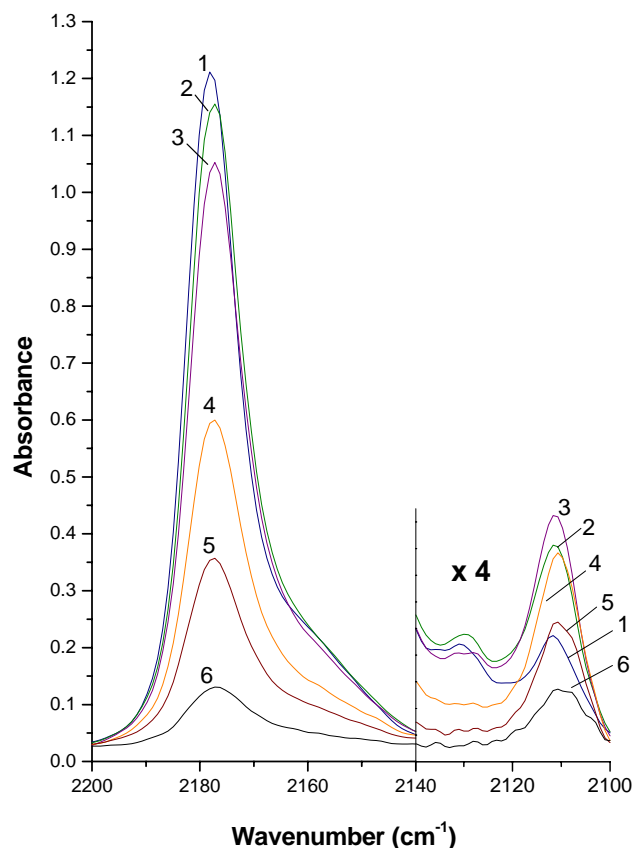


Figure 1. Selected spectra of CO (*ca.* 1.5 Torr) adsorbed on Na-ZSM-5 at variable temperature: (1) 123 K; (2) 143 K; (3) 163 K; (4) 243 K; (5) 263 K; (6) 293 K.

A very weak IR absorption band, at about 2130 cm^{-1} , is also observed in the low temperature spectra of Figure 1. Its intensity gradually decreases when temperature is raised, showing the same behaviour as that of the HF band. This band at 2130 cm^{-1} has a bathochromic shift of 48 cm^{-1} , referred to the HF band, which is exactly the isotopic shift value expected on substituting ^{12}C by ^{13}C ; hence, the 2130 cm^{-1} band clearly corresponds to the ^{13}CO counterpart (natural abundance about 1%) of the HF band at 2178 cm^{-1} . It is also relevant to say that the Na-ZSM-5 zeolite used showed the expected silanol band at 3744 cm^{-1} . This silanol band was only very slightly affected by adsorbed carbon monoxide. The corresponding effect in the C–O stretching region is shown in the low frequency tail of the main band at 2178 cm^{-1} (Figure 1); this effect was allowed for when measuring the integrated intensity of the HF band.

Some variable-temperature IR spectra of CO adsorbed on Na-Y are shown in Figure 2. The HF band (C–O stretching of $\text{Na}^+\cdots\text{CO}$ adducts) appears at 2171 cm^{-1} , while the LF band ($\text{Na}^+\cdots\text{OC}$ species) is seen at 2122 cm^{-1} . These bands display the same temperature dependence as already seen for the CO/Na-ZSM-5 system; when temperature is increased the HF band decreases continuously, while the LF band first increases and then decreases. Qualitatively, the same behaviour was also observed for carbon monoxide adsorbed on K-ZSM-5 [34] and on Rb-ZSM-5 [35]. In all cases,

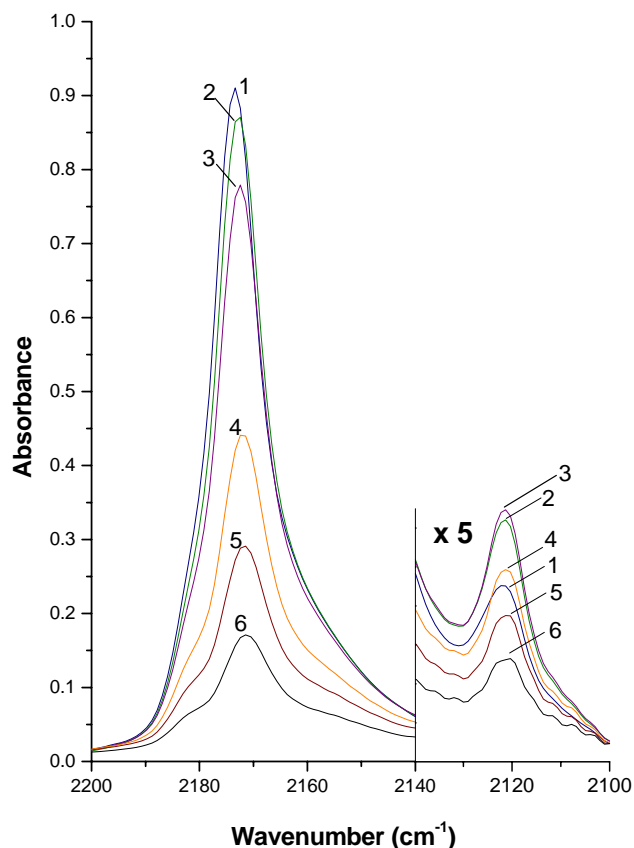


Figure 2. Selected spectra of CO (*ca.* 1.5 Torr) adsorbed on Na-Y at variable temperature: (1) 167 K; (2) 187 K; (3) 197 K; (4) 215 K; (5) 225 K; (6) 233 K.

$M^+ \cdots CO$ and $M^+ \cdots OC$ species were found to be inter-related by the temperature-dependent equilibrium described by Equation (1).

As shown below, the intensity ratio between LF and HF bands should be proportional to the equilibrium constant for the isomerization process described by Equation (1). Hence, the representation of the natural logarithm of this intensity ratio, $\ln (A_{LF}/A_{HF})$, versus reciprocal temperature, $1/T$, constitutes the corresponding van't Hoff plot. These plots are reported in Figure 3 for all systems studied. From the slope of the straight lines, corresponding values of ΔH° were derived. These values are summarized in Table 1, which also gives the position of the corresponding HF and LF bands.

3. Outline of Quantum Chemical Studies

Ferrari *et al.* [23] and Ugliengo *et al.* [28] carried out detailed quantum chemical calculations on the interaction between CO and bare alkali-metal cations, both at the SCF level and by using a density functional method at the B3-LYP level. This last method combines a Becke's hybrid exchange functional (which contains a tuned fraction of Hartree-Fock exchange) with the Lee, Yang and Parr gradient-corrected correlation functional. Results from B3-LYP calculations will be the only ones

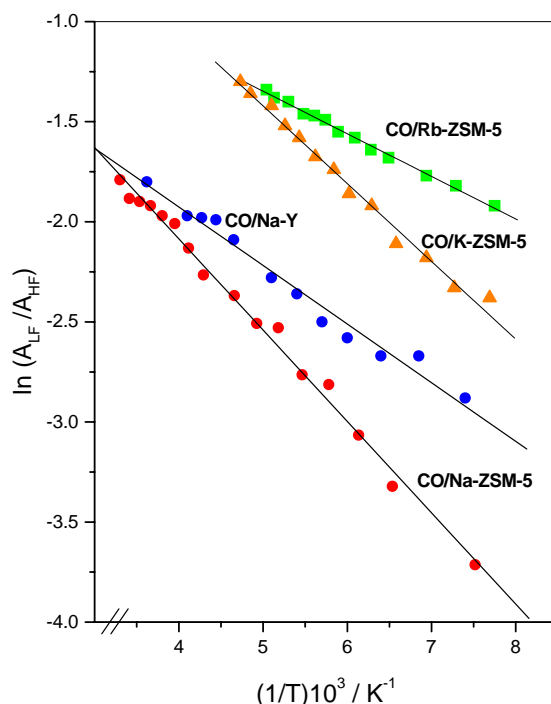


Figure 3. The van't Hoff plots of the natural logarithm of the intensity ratio for LF and HF bands vs. reciprocal temperature.

Table 1. Peak position of the HF and LF bands, and ΔH° values derived from the corresponding van't Hoff plots.

System	$\nu(\text{HF})$, cm^{-1}	$\nu(\text{LF})$, cm^{-1}	ΔH° , kJ mol^{-1}
CO/Na-ZSM-5	2178	2112	3.8
CO/K-ZSM-5	2166	2117	3.2
CO/Rb-ZSM-5	2161	2120	1.8
CO/Na-Y	2171	2122	2.4

considered here, since they turned out to be more reliable than those obtained by using SCF methods [23,28].

Compared to the situation arising when CO is adsorbed on alkali-metal-exchanged zeolites, the bare cation model is rather crude, since it ignores the effect of the negatively charged zeolite framework. However, the main observed features of the cation-CO interaction were reproduced quite satisfactorily. $\text{M}(\text{CO})^+$ and $\text{M}(\text{OC})^+$ species were both found to have a smaller energy than the corresponding unbound systems, and C-bonded species were found to involve a higher interaction energy than O-bonded adducts. Correct signs of the C–O stretching frequency shifts (upward for $\text{M}(\text{CO})^+$ and downward for $\text{M}(\text{OC})^+$ species) were deduced, and trends in binding energy were found

to be in agreement with experimental results. The conclusion was [28] that the bare cation model can be used (as a first approximation) for analysing the interaction of CO with alkali-metal cations in zeolites, the absence of nearby oxide anions notwithstanding.

In order to allow for effects due to the zeolite framework, calculations were also performed (at the B3-LYP level) on the interaction between CO and the cluster model $[\text{AlH}(\text{OH})_3]\text{M}^+$ (M= Li, Na, K, Rb, Cs) which contains three oxygen atoms in the immediate neighbourhood of the alkali-metal cation [29]. Comparison between the results obtained by using this minimal cluster model and those calculated for bare cations showed [28] that presence of the anionic species considerably reduces the cation-CO interaction energy, and brings computed data closer to experimental results in what concerns both the stretching C–O frequency and the binding energy.

When comparing ab-initio calculations with experimental results, the most significant observable is the standard enthalpy difference, ΔH° , between the C-bonded $\text{M}(\text{CO})^+$ and the O-bonded $\text{M}(\text{OC})^+$ species. Table 2 summarizes the computational results obtained by using both, the bare cation and the $[\text{AlH}(\text{OH})_3]\text{M}^+$ cluster models. To facilitate comparison, the experimental results obtained for alkali-metal-exchanged ZSM-5 zeolites are also included in this table.

Table 2. Enthalpy change (kJ mol^{-1}) in the isomerization process $\text{ZM}(\text{CO})^+ \rightleftharpoons \text{ZM}(\text{OC})^+$.

M^+	$\Delta H^\circ/\text{bare cation}$	$\Delta H^\circ/[\text{AlH}(\text{OH})_3]\text{M}^+$	$\Delta H^\circ/\text{experimental}$
Li^+	16.3	6.3	-
Na^+	12.2	5.6	3.8
K^+	6.3	2.9	3.2
Rb^+	5.4	2.5	1.8
Cs^+	4.6	2.1	-

4. Discussion

4.1 Thermal isomerization equilibrium

The infrared spectroscopic results reviewed here prove that when C-bonded $\text{M}(\text{CO})^+$ species are formed by adsorbing CO on alkali-metal-exchanged zeolites, they are in thermal equilibrium with O-bonded $\text{M}(\text{OC})^+$ species; which is also in agreement with quantum chemical calculations on model systems. Such a thermal isomerization equilibrium is clearly demonstrated by the observed linear dependence (Figure 3) of the natural logarithm of the intensity ratio, $A_{\text{LF}}/A_{\text{HF}}$, versus $1/T$; which is precisely the behaviour to be expected for the linkage isomerization equilibrium described by equation (1). The equilibrium constant, K , of this equation should be equal to the ratio $\theta_{\text{OC}}/\theta_{\text{CO}}$, where θ_{OC} and θ_{CO} are the fractional coverages of O-bonded and C-bonded carbonyls, respectively. Consequently, if

$\epsilon_{\text{HF}}/\epsilon_{\text{LF}}$ is the ratio of molar absorption coefficients of the corresponding infrared absorption bands, we have,

$$K = (A_{\text{LF}}/A_{\text{HF}})(\epsilon_{\text{HF}}/\epsilon_{\text{LF}}) \quad (2)$$

The temperature dependence of K is given by the van't Hoff equation:

$$\ln K = (-\Delta H^\circ/RT) + (\Delta S^\circ/R) \quad (3)$$

Combination of equations (2) and (3) yields:

$$\ln (A_{\text{LF}}/A_{\text{HF}}) = (-\Delta H^\circ/RT) + (\Delta S^\circ/R) + \ln (\epsilon_{\text{HF}}/\epsilon_{\text{LF}}) \quad (4)$$

Therefore, the standard enthalpy change, ΔH° , involved in the linkage isomerization equilibrium between C-bonded, $\text{M}(\text{CO})^+$, and O-bonded, $\text{M}(\text{OC})^+$, species can be directly obtained (Table 1) from the van't Hoff plots shown in Figure 3, without a need to know the corresponding values of ϵ_{LF} and ϵ_{HF} . It should be noted, however, that correct application of the van't Hoff equation demands constant values of ΔH° and ΔS° over the whole temperature range involved. Fulfilment of these requirements can be assumed from the fact that quantum chemical calculations on model systems [23,28] have shown that ΔC_p° for the equilibrium process described in equation (1) is negligible. Hence ΔH° and ΔS° should be (to a good approximation) temperature independent, since these parameters are related to ΔC_p° through the well known thermodynamic equations:

$$d\Delta H^\circ/dT = \Delta C_p^\circ \quad (5)$$

and

$$d\Delta S^\circ/dT = \Delta C_p^\circ/T \quad (6)$$

It is also relevant to add that computations performed by using the model cluster $[\text{AlH}(\text{OH})_3]^- \text{M}^+$ have shown [29] that the value of $T\Delta S^\circ$, at 77 K, to be expected for the isomerization equilibrium between C-bonded and O-bonded carbonyls is always smaller than 0.4 kJ mol^{-1} regardless of which alkali-metal cation is considered.

The experimental values of the isomerization enthalpy (Table 2) are lower than those calculated by using the bare cation model. This should be expected, since the computational model does not take into account nearby oxygen anions in the zeolite framework. Computational results obtained by using the $[\text{AlH}(\text{OH})_3]^- \text{M}^+$ cluster give ΔH° values closer to those experimentally measured.

4.2 Isomerization enthalpy as a function of electric field

When CO interacts through its carbon atom with a positively charged centre, the electrostatic field increases the C–O stretching force constant and decreases the bond length [30]. Consequently, the C–O stretching frequency becomes higher than the 2143 cm^{-1} value for free carbon monoxide. The magnitude of this hypsochromic shift can be used for calculating the corresponding electric field

[22,30]. For CO adsorbed on alkali-metal-exchanged zeolites, experimental values of $\nu(\text{HF})$ were used to determine the magnitude of the axial electric field, E , set by the cation (and nearby framework anions) at the centre of the adsorbed CO molecule. Values were found to range from 2.4 V nm^{-1} for Cs-ZSM-5 up to 9.5 V nm^{-1} for Li-ZSM-5 [2,20]. For the faujasite-type M^+ -Y zeolites, smaller values of E were obtained for the same cations. This is due to the fact [13] that in faujasites the extra-framework cation has more (negatively charged) framework oxygen neighbours than in ZSM-5 zeolites. Note, in this context, that $\nu(\text{HF})$ takes the value of 2178 cm^{-1} for CO/Na-ZSM-5 while it is only 2171 cm^{-1} for CO/Na-Y (Table 1). Knowledge of the electric field allows a correlation between E and ΔH° (the isomerization enthalpy of $M(\text{CO})^+/M(\text{OC})^+$ species) to be analysed.

Figure 4 shows the plot of ΔH° against E for both the computational results obtained with the $[\text{AlH}(\text{OH})_3]M^+$ cluster (which most closely approach those found experimentally) and the experimental values of isomerization enthalpy. It is seen that an approximately linear correlation is obtained in both cases. The basis for such a correlation is as follows. The potential energy, V , of a dipole (the CO molecule) in an external electric field, E , is given by:

$$V = -\mu E \quad (\mu: \text{dipole moment}) \quad (7)$$

As a first approximation, reversing the orientation of the dipole in the electric field should involve an energy difference twice as much as that given by equation (7), and this energy difference should be nearly equal to ΔH° . Hence, to a first approximation, we have:

$$\Delta H^\circ = 2\mu E, \quad (8)$$

which justifies the linear plots in Figure 4. It should be noted that none of the lines in these plots goes exactly through the origin of coordinates, but differences are small. Referring to experimental data (bottom plot in Figure 4) the vertical intercept of the linear plot amounts to only $+0.39 \text{ kJ mol}^{-1}$, which is about the order of magnitude of the accuracy with which experimental values of ΔH° are determined [35], and one should also consider the approximate character of equation (8). It should be noted, in particular, that bonding through the oxygen instead of through the carbon atom can result in a different cation-CO equilibrium distance, and this would lead to a different E value at the centre of the CO molecule. For the case of the plot obtained from computational values of ΔH° (Figure 4), the vertical intercept of the straight line could also have a contribution from the fact that E values in the abscissa are those estimated for intrazeolite electric fields [2,20], and not those corresponding to the computational cluster model actually used. This fact could also slightly affect the slope of the ΔH° versus E straight line.

By using equation (8), the experimental results in Figure 4 (bottom plot) can be used to derive an approximate value for the dipole moment of the CO molecule. The slope of the straight line (2μ) is 0.50 , in units of $\text{kJ mol}^{-1} \text{ V}^{-1} \text{ nm}$. Conversion into appropriate units leads to $\mu = 0.42 \cdot 10^{-30} \text{ C m}$, which is remarkably close to the well known value [31,39] of $\mu = 0.37 \cdot 10^{-30} \text{ C m}$ (*i.e.*, 0.11 D). This finding suggests that, regardless of its approximate character, the experimentally derived linear plot can be

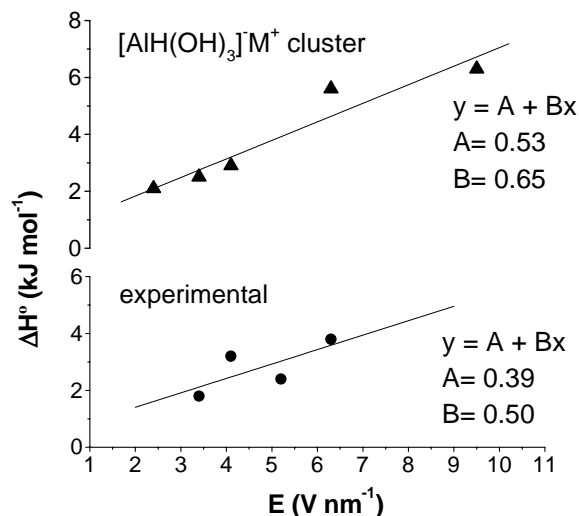


Figure 4. Plots of isomerization enthalpy versus electric field.

used to estimate ΔH° from corresponding E values; and hence from $\nu(\text{HF})$. It should be acknowledged, however, that more experimental values of ΔH° for different zeolites and cations are desirable, in order to refine the model and to establish general trends more firmly.

5. Conclusions and outlook

Both quantum chemical calculations and experimental results obtained by variable temperature FTIR spectroscopy prove that $\text{M}(\text{CO})^+$ and $\text{M}(\text{OC})^+$ species, formed when CO is adsorbed on alkali-metal-exchanged zeolites, are in a thermal isomerization equilibrium. The corresponding isomerization enthalpy, ΔH° , depends on both the cation considered and the zeolite structure type. To a first approximation, ΔH° was found to be a linear function of the electric field created by the cation and nearby oxygen atoms in the zeolite framework. An approximate value of ΔH° can be derived from a simple electrostatic model which considers the energy involved in reversing the orientation of the dipolar CO molecule in the corresponding electric field; it should be noted, however, that this fact was proved for only a few cases. Measurements on other cations and zeolites are desirable, in order to test conclusions to a larger extent.

Finally, it should be pointed out that linkage isomerism, as found for carbon monoxide, could also be displayed by other heteroatomic molecules, such as NO or N_2O . Indeed, there is some evidence [40] that nitric oxide can coordinate extra-framework cations in zeolites forming both N-bonded and O-bonded adducts, but no detailed studies on this molecule are yet available. This research field, which is of considerable interest regarding both theoretical aspects of coordination chemistry and practical uses of zeolites, deserves further development. It is hoped that the interplay between experimental research

and quantum chemical calculations, much in the same way as shown in this review, will continue to yield fruitful results.

References

1. Cohen de Lara, E.; Nguyen Tan, T. Potential energy of a molecule adsorbed in synthetic zeolites. Application to the analysis of infrared spectra. 1. Electrostatic field in the zeolites NaA and CaA. *J. Phys. Chem.* **1976**, *80*, 1917-1921.
2. Otero Areán, C. Zeolites and intrazeolite chemistry: insights from infrared spectroscopy. *Comments Inorg. Chem.* **2000**, *22*, 241-273.
3. Makarova, M. A.; Al-Ghefaily, K. M.; Dwyer, J. Brønsted acid strength in US-Y: FTIR study of CO adsorption. *J. Chem. Soc. Faraday Trans.* **1994**, *90*, 383-386.
4. Gruver, V.; Fripiat, J. J. Lewis acid sites and surface aluminum in aluminas and mordenites: an infrared study of CO chemisorption. *J. Phys. Chem.* **1994**, *98*, 8549-8554.
5. Bordiga, S.; Garrone, E.; Lamberti, C.; Zecchina, A.; Otero Areán, C.; Kazansky, V. B.; Kustov, L. M. Comparative IR spectroscopic study of low temperature H₂ and CO adsorption on Na zeolites. *J. Chem. Soc. Faraday Trans.* **1994**, *90*, 3367-3372.
6. Wakabayashi, F.; Kondo, J. N.; Domen, K.; Hirose, C. Direct comparison of N₂ and CO as IR spectroscopic probes of acid sites in H-ZSM-5 zeolite. *J. Phys. Chem.* **1995**, *99*, 10573-10580.
7. Borovkov, V. Yu.; Karge, H. G. Use of combination modes and overtones of metal carbonyls for the IR study of cation states in zeolites. *J. Chem. Soc. Faraday Trans.* **1995**, *91*, 2035-2039.
8. Lercher, J. A.; Gründling, C.; Eder-Mirth, G. Infrared studies of the surface acidity of oxides and zeolites using adsorbed probe molecules. *Catal. Today* **1996**, *27*, 353-376.
9. Zecchina, A.; Otero Areán, C. Diatomic molecular probes for Mid-IR studies of zeolites. *Chem. Soc. Rev.* **1996**, *25*, 187-197.
10. Lavalley, J. C. Infrared spectrometric studies of the surface basicity of metal oxides and zeolites using adsorbed probe molecules. *Catal. Today* **1996**, *27*, 377-401.
11. Otero Areán, C.; Turnes Palomino, G.; Escalona Platero, E.; Peñarroya Mentrut, M. Zeolite-supported metal carbonyls: sensitive probes for infrared spectroscopic characterization of the zeolite surface. *J. Chem. Soc. Dalton Trans.* **1997**, 873-879.
12. Onida, B.; Gabelica, Z.; Lourenço, J. P.; Ribeiro, M. F.; Garrone, E. Spectroscopic characterization of the hydroxyl groups in SAPO-40. 2. Interaction with CO and N₂. *J. Phys. Chem. B* **1997**, *101*, 9244-9249.
13. Knözinger, H.; Huber, S. IR spectroscopy of small and weakly interacting molecular probes for acidic and basic zeolites. *J. Chem. Soc. Faraday Trans.* **1998**, *94*, 2047-2059.
14. Katoh, M.; Yamazaki, T.; Ozawa, S. IR spectroscopic study of adsorption of binary gases over ion-exchanged ZSM-5 zeolites. *J. Colloid Interf. Sci.* **1998**, *203*, 447-455.
15. Li, P.; Xiang, Y.; Grassian, V. H.; Larsen, S. C. CO adsorption as a probe of acid sites and the electric field in alkaline earth exchanged zeolite beta using FTIR and ab initio quantum calculations. *J. Phys. Chem. B* **1999**, *103*, 5058-5062.

16. Otero Areán, C.; Turnes Palomino, G.; Zecchina, A.; Spoto, G.; Bordiga, S.; Roy, P. Cation-carbon stretching vibration of adducts formed upon CO adsorption on alkaline zeolites. *Phys. Chem. Chem. Phys.* **1999**, *1*, 4139-4140.
17. Otero Areán, C.; Turnes Palomino, G.; Zecchina, A.; Bordiga, S.; Llabrés i Xamena, F. X.; Pazè, C. Vibrational spectroscopy of carbon monoxide and dinitrogen adsorbed on magnesium-exchanged ETS-10 molecular sieve. *Catal. Lett.* **2000**, *66*, 231-235.
18. Hadjiivanov, K.; Knözinger, H.; Ivanova, E.; Dimitrov, L. FTIR study of low-temperature CO and $^{15}\text{N}_2$ adsorption on a CaNaY zeolite: formation of site-specific $\text{Ca}^{2+}(\text{CO})_3$ and $\text{Ca}^{2+}(^{15}\text{N}_2)_3$ complexes. *Phys. Chem. Chem. Phys.* **2001**, *3*, 2531-2536.
19. Otero Areán, C.; Manoilova, O. V.; Rodríguez Delgado, M.; Tsyganenko, A. A.; Garrone, E. Formation of several types of coordination complexes upon CO adsorption on the zeolite Li-ZSM-5. *Phys. Chem. Chem. Phys.* **2001**, *3*, 4187-4188.
20. Garrone, E.; Rodríguez Delgado, M.; Otero Areán, C. Trends in infrared spectroscopy of zeolites. *Trends Inorg. Chem.*, in press.
21. Zecchina, A.; Bordiga, S.; Lamberti, C.; Spoto, G.; Carnelli, L.; Otero Areán, C. Low-temperature Fourier transform infrared study of the interaction of CO with cations in alkali-metal-exchanged ZSM-5 zeolites. *J. Phys. Chem.* **1994**, *98*, 9577-9582.
22. Pacchioni, G.; Cogliandro, G.; Bagus, P. S. Molecular orbital cluster model study of bonding and vibrations of CO adsorbed on MgO surfaces. *Int. J. Quantum Chem.* **1992**, *42*, 1115-1139.
23. Ferrari, A. M.; Ugliengo, P.; Garrone, E. Ab initio study of the adducts of carbon monoxide with alkaline cations. *J. Chem. Phys.* **1996**, *105*, 4129-4139.
24. Böse, H.; Förster, H. Sorption states of isoelectronic linear molecules in zeolites. *J. Mol. Struct.* **1990**, *218*, 393-398.
25. Katoh, M.; Yamazaki, T.; Ozawa, S. IR spectra for adsorbed CO on various alkali metal ion-exchanged ZSM-5 zeolites. *Bull. Chem. Soc. Jpn.* **1994**, *67*, 1246-1253.
26. Turnes Palomino, G.; Otero Areán, C.; Geobaldo, F.; Ricchiardi, G.; Bordiga, S.; Zecchina, A. FTIR study of CO adsorbed at low temperature on zeolite L. Evidence for an ordered distribution of aluminium atoms. *J. Chem. Soc. Faraday Trans.* **1997**, *93*, 189-191.
27. Garrone, E.; Fubini, B.; Bonelli, B.; Onida, B.; Otero Areán, C. Thermodynamics of CO adsorption on the zeolite Na-ZSM-5. A combined microcalorimetric and FTIR spectroscopic study. *Phys. Chem. Chem. Phys.* **1999**, *1*, 513-518.
28. Ugliengo, P.; Garrone, E.; Ferrari, A. M.; Zecchina, A.; Otero Areán, C. Quantum chemical calculations and experimental evidence for O-bonding of carbon monoxide to alkali metal cations in zeolites. *J. Phys. Chem. B* **1999**, *103*, 4839-4846.
29. Ferrari, A. M.; Neyman, K. M.; Rösch, N. CO interaction with alkali metal cations in zeolites: A density functional model cluster study. *J. Phys. Chem. B* **1997**, *101*, 9292-9298.
30. Hush, N. S.; Williams, M. L. Carbon monoxide bond length, force constant and infrared intensity variations in strong electric fields: Valence-shell calculations with applications to properties of adsorbed and complexed CO. *J. Mol. Spectrosc.* **1974**, *50*, 349-368.

31. Larsson, R.; Lykvist, R.; Rebenstorf, B. On the IR frequency shift of carbon monoxide adsorbed on positive surface ions. *Z. Phys. Chem., Leipzig* **1982**, *263*, 1089-1104.
32. Lupinetti, A. J.; Strauss, S. H.; Frenking, G. Nonclassical metal carbonyls. *Progr. Inorg. Chem.* **2001**, *49*, 1-112.
33. Otero Areán, C.; Tsyganenko, A. A.; Escalona Platero, E.; Garrone, E.; Zecchina, A. Two coordination modes of CO in zeolites: A temperature-dependent equilibrium. *Angew. Chem. Int. Ed.* **1998**, *37*, 3161-3163.
34. Manoilova, O. V.; Peñarroya Mentrut, M.; Turnes Palomino, G.; Tsyganenko, A. A.; Otero Areán, C. Variable-temperature infrared spectrometry of carbon monoxide adsorbed on the zeolite K-ZSM-5. *Vib. Spectrosc.* **2001**, *26*, 107-111.
35. Otero Areán, C.; Peñarroya Mentrut, M.; Rodríguez Delgado, M.; Turnes Palomino, G.; Manoilova, O. V.; Tsyganenko, A. A.; Garrone, E. Variable temperature FTIR spectroscopy of carbon monoxide adsorbed on protonic and rubidium-exchanged ZSM-5 zeolites. *Stud. Surf. Sci. Catal.*, in press.
36. Tsyganenko, A. A.; Escalona Platero, E.; Otero Areán, C.; Garrone, E.; Zecchina, A. Variable-temperature IR spectroscopic studies of CO adsorbed on Na-ZSM-5 and Na-Y zeolites. *Catal. Lett.* **1999**, *61*, 187-192.
37. Szostak, R. *Molecular Sieves*, Van Nostrand Reinhold, New York, 1989.
38. Otero Areán, C.; Manoilova, O. V.; Tsyganenko, A. A.; Turnes Palomino, G.; Peñarroya Mentrut, M.; Geobaldo, F.; Garrone, E. Thermodynamics of hydrogen bonding between CO and the supercage Brønsted acid sites of the H-Y zeolite: Studies from variable temperature IR spectroscopy. *Eur. J. Inorg. Chem.* **2001**, 1739-1743.
39. Muenter, J. S. Electric dipole moment of carbon monoxide. *J. Mol. Spectrosc.* **1975**, *55*, 490-491.
40. Zecchina, A.; Otero Areán, C.; Turnes Palomino, G.; Geobaldo, G.; Lamberti, C.; Spoto, G.; Bordiga, S. The vibrational spectroscopy of H₂, N₂, CO and NO adsorbed on the titanosilicate molecular sieve ETS-10. *Phys. Chem. Chem. Phys.* **1999**, *1*, 1649-1657.